Understanding opalescence measurements of biologics: a comparison study of methods, standards, and molecules

Kunz, P.; Stuckenberger, E.; Hausmann, K.; Gentiluomo, L.; Neustrup, M.; Michalakis, S.; ... ; Menzen, T.

International Journal of Pharmaceutics 628 (2022) 122321

Contents lists available at ScienceDirect

International Journal of Pharmaceutics

journal homepage: www.elsevier.com/locate/ijpharm

Understanding opalescence measurements of biologics – A comparison study of methods, standards, and molecules

Patrick Kunz [a], Eva Stuckenberger [a], Kerstin Hausmann [a], Lorenzo Gentiluomo [a], Malene Neustrup [b], Stylianos Michalakis [c], Ruth Rieser [d], Stefan Romeijn [e], Christian Wichmann [f], Roland Windisch [f], Andrea Hawe [a], Wim Jiskoot [a,e,1], Tim Menzen [a,*]

[a] Coriolis Pharma Research GmbH, Martinsried, Germany
[b] Leiden University, Division of Drug Delivery Technology, Leiden Academic Centre for Drug Research, Leiden, The Netherlands
[c] Department of Ophthalmology, University Hospital, LMU Munich, Munich, Germany
[d] Department of Pharmaceutical Technology and Biopharmaceutics, LMU Munich, Munich, Germany
[e] Leiden University, Division of BioTherapeutics, Leiden Academic Centre for Drug Research, Leiden, The Netherlands
[f] Department of Transfusion Medicine, Cell Therapeutics and Hemostaseology, University Hospital, LMU Munich, Munich, Germany

ARTICLE INFO

Keywords:
Opalescence
Nephelometry
Turbidity
Light scattering
Biopharmaceuticals
Gene and cell therapy products

ABSTRACT

Opalescence measurements are broadly applied to assess the quality and stability of biopharmaceutical products at all stages of development and manufacturing. They appear to be simple and straight forward but detect complex light scattering phenomena. Despite a routine calibration step, opalescence values obtained with the same biopharmaceutical sample but on different instruments and/or with different methods may vary significantly. Since the reasons for this high variability are generally not well understood, comparison of opalescence results from different biopharmaceutical laboratories is difficult. Here, we characterized a comprehensive set of biopharmaceutically relevant samples with five opalescence methods to illustrate fundamental differences in method performance and explore the reasons for poor comparability. In addition, we developed a high-throughput method for measuring opalescence in a conventional light scattering plate reader that yields opalescence values in the same range as compendial methods. The presented results underline the impact of sample properties, instrument type, and calibration standards on the determined opalescence value. Based on our findings we provide recommendations for the appropriate application of each method during biopharmaceutical drug product development. Overall, our study contributes to an improved understanding of opalescence measurements in the biopharmaceutical field.

1. Introduction

Opalescence measurements are routinely applied to characterize the optical appearance of biopharmaceutical products and advanced therapy medicinal products (ATMPs). As a stability-indicating parameter, opalescence can reveal unfavorable product-related properties and time-dependent changes. For instance, protein aggregation can lead to particulate impurities that increase opalescence (Raut and Kalonia, 2015b; Sukumar et al., 2004; Yang, 2016). Moreover, opalescence can be observed in case of high protein concentrations as a characteristic property of the product (Mason et al., 2011; Raut and Kalonia, 2015a; Yang, 2016). Similarly, particulate biopharmaceutical formulations may show opalescence as an intrinsic attribute of their particulate nature, for instance the prominent COVID-19 vaccines such as mRNA lipid nanoparticle vaccines (BioNTech; BioNTech; Moderna), as well as the viral vector-based vaccines (AstraZeneca; Janssen). Consequently, opalescence measurements are particularly useful not only during quality control testing but also during various stages of product development, e.g., upstream processing or formulation development.

Opalescence measurements appear to be remarkably simple and straight forward, however, rely on extraordinarily complex optical properties of the respective sample and the employed instrumentation. Substantial complications arise from a diverse terminology that uses “opalescence”, “turbidity”, “opacity” or “cloudiness” synonymously, as

* Corresponding author.
E-mail address: Tim.Menzen@coriolis-pharma.com (T. Menzen).
[1] In Memoriam of our valued colleague and friend Wim Jiskoot who contributed to this manuscript and tragically passed away.

https://doi.org/10.1016/j.ijpharm.2022.122321
Received 8 April 2022; Received in revised form 14 October 2022; Accepted 15 October 2022
Available online 20 October 2022

well as from numerous measurement principles and possible instrument settings, resulting in an array of corresponding measurement units.

Commonly, the terms "opalescence" and "turbidity" are used synonymously in the biopharmaceutical field. Although the term "opalescence" originally refers to the changing colors of an opal (Oxford Advanced Learner's Dictionary, 2020), both terms address a slightly blueish to whitish, or cloudy appearance of a solution that indicates increased light scattering, originating from phenomena like aggregation, fluctuations in concentration that lead to liquid–liquid phase separation, reversible self-association of proteins, as well as gelation (Mason et al., 2011; Raut and Kalonia, 2015a, 2015b; Rogers et al., 2019; Sukumar et al., 2004). In very simple terms, "turbidity is the opposite of clarity" (Sadar).

Nephelometry and turbidimetry represent the two major measurement principles for opalescence. In the non-ratio mode, nephelometry detects light scattering at a 90° angle from the incoming beam, as it is realized in conventional nephelometers or fluorescence spectrometers and which is particularly suited for low opalescence values. In nephelometry's ratio mode, additional detectors are placed at 0° (forward scattering or transmission signal; Note: other literature might refer to this configuration as 180°) or further scattering angles, to detect and correct potential artefacts that originate from sample coloration. In turbidimetry the transmission signal at a scattering angle of 0° is detected, thereby quantifying the reduction of light intensity of the incoming beam that is caused by light scattering, as well as potential absorbance. Notably, regulatory monographs like the European Pharmacopoeia (Ph. Eur.) leave considerable room for further measurement modes besides nephelometry and turbidimetry, in principle allowing to employ diverse scattering angles and wavelengths of light (10th European Pharmacopoeia (Ph.Eur.10), 2020).

Numerous opalescence units exist that arise from the applied measurement principle and method specification, which were standardized by the ASTM (American Society for Testing And Materials) in the standard document D7315 (ASTM D7315-17, 2018). Nephelometric turbidity units (NTU) and formazin nephelometric units (FNU) apply only for 90° measurement setups when using a white light source (400–600 nm) according to US specification Method 180.1 (Method 180.1, 1993) and a monochromatic light source in the range between 780 and 900 nm (e.g., 860 nm in case of the non-ratio nephelometer) according to EU specification ISO 7027 (ISO 7027–1:2016, 2016), respectively. When the ratio-mode is used, ASTM also differentiates nephelometric turbidity ratio units (NTRU) and formazin nephelometric ratio units (FNRU). The opalescence in 0° (transmission) and 90-180° setups is measured in formazin attenuation units (FAU) and formazin backscatter units (FBU), respectively.

To ensure comparability between opalescence measurements, both nephelometry and turbidimetry analyses require calibration with a primary standard. Originally developed for water quality testing, a 4000 NTU formazin standard suspension is the sole available primary standard. It can be reproducibly prepared by using traceable components and is diluted to generate further calibration points. Surprisingly, key properties of formazin such as particle size distribution, angular dependent scattering properties and its refractive index, are not well established in the literature, despite of its important role for measuring opalescence (Münzberg et al., 2017). Alternative standards are generally accepted and used for calibration, including suspensions of stabilized formazin, which offer a much-improved shelf life, but also polymer-based standards, usually consisting of styrene divinylbenzene microspheres. Finally, secondary standards mimic the behavior of the primary standard, but only for well-defined instrument settings. They are used to confirm successful calibration with the primary standard by serving as a system suitability test. Consequently, different calibration standards are available with sparse information about their specific light scattering properties and respective instrument suitability. In their excellent study, Barros and colleagues indicated that the methodological diversity causes poor inter-laboratory comparability of opalescence measurements, representing a serious consequence of this methodological diversity and that a knowledge gap regarding the impact of samples, instruments, units and standards is prevalent in the biopharmaceutical field (Barros et al., 2021). Our work aims at further closing this knowledge gap by providing a comprehensive comparison of diverse methods in the context of a large set of biopharmaceutical samples and the usage of different calibration standards.

In particular, we involved two aged protein drug products (erythropoietin and the fusion protein abatacept), two virus materials (adeno-associated virus and Sendai virus), liposomes, poly(lactic-*co*-glycolic acid) (PLGA) nanoparticles, alum particles (aluminum hydroxide, typically used as adjuvants) and a Jurkat cell sample (as a model for cell-based medicinal products). By this selection, different chemistries like amino acids, nucleic acids, lipids, and metals were included (Table 2). Importantly, since parameters like molecular size, shape, polarizability and the underlying particle distribution largely determine the optical properties of a solution or suspension, a broad size range from few nanometers to several micrometers was covered, as well as different molecular shapes and size distributions. Due to this variety of molecular properties, the employed collection of products formed a relevant set for a comprehensive comparison of common opalescence methods in a sample-dependent manner.

To instrumentally determine opalescence, a selection of instruments was chosen that covered the most conventional opalescence measurement setups. The selection of systems was highly diverse in the detection mode (scattered versus transmitted light), in the detection angle and detector type, as well as in the light source and the employed wavelength range of the incident light beam (Table 1). Two cuvette-based systems were employed, including a frequently used ratio nephelometer, as well as a non-ratio nephelometer. Furthermore, a microplate nephelometer was included that detects forward scattering up to a scattering angle of 80°, whereas an absorbance plate reader represented the principle of turbidimetry by measuring the transmission signal at 0°. In comparison, visual inspection according to Ph. Eur. was performed to assess the samples' opalescence semi-quantitatively by the naked eye, followed by the instrumental determination of sample color according to Ph. Eur. Finally, we developed a novel low-volume, high-throughput method for opalescence analysis by using static light scattering in a conventional microplate reader.

2. Material & methods

2.1. Sample materials

Expired Retacrit 40,000 IE prefilled syringes and expired Orencia 125 mg pens were used to obtain aged erythropoietin (epo) and aged abatacept, respectively. PLGA nanoparticles were prepared with a microfluidic setup. The system consisted of two syringes, where one syringe contained PLGA (acid terminated, lactide:glycolide 50:50, Mw 24,000–38,000; purchased from Sigma-Aldrich Chemie B.V. (Zwijndrecht, the Netherlands)) dissolved in acetonitrile and the second syringe ultrapure water with the surfactant poly(vinyl alcohol) (Mw ~ 31,000; purchased from Sigma-Aldrich Chemie B.V. (Zwijndrecht, the Netherlands)). The liquids in the syringes were pumped into a microfluidic setup where the fluids met in a co-flow. After preparation, the organic solvent was evaporated under a stream of nitrogen and the final concentration of 0.18 mg/ml was adjusted by dilution with water. Cationic liposomes (DOTAP:DOPC, 1:1 molar ratio) were produced on a small scale, 500 µl – 2 ml per batch, by making use of the thin film dehydration-rehydration method as previously described (Heuts et al., 2018). After hydration of the dry lipid film with ultrapure water the suspension was freeze-dried overnight in a Christ alpha 1–2 freeze-dryer (Osterode, Germany). The following day the lipid cake was rehydrated with 10 mM sodium phosphate buffer at pH 7.4 in three consecutive steps: twice the addition of 25 % of the final volume (30 min equilibration after each addition) and as a third step the remaining 50 % of the

Table 1
Overview of instruments used in this study to characterize various biopharmaceutical samples, together with their respective parameters, settings, exemplary calibration curve, and correct technical turbidity unit (TU).

Instrument	Instrument parameters					Measurement settings		Instrument calibration	
	Detection mode	Measurement angle(s)	Detector	Light source	Unit	Sample cell	Sample volume	Calibration curve [TU]	R^2
Ratio nephelometer (HACH 2100AN)	Light scattering	0°, 30°, 90°, 138°	Photodiode	Tungsten lamp, 400 – 600 nm filter	NTRU NTU-RATIO	Glass test tube	2 ml	0 – 100	1.000
Non-ratio nephelometer (NEPHLA)	Light scattering	90°	Photodiode	LED, 860 ± 60 nm	FNU	Glass test tube	2 ml	0 – 100	0.999
Microplate nephelometer (NEPHELOstar)	Light scattering	0 – 80°	Side window photodiode detector	Self-monitoring laser diode, 635 ± 10 nm	TU	96-well plate	200 µl	0 – 100	0.998
Absorbance plate reader (neo2)	Light transmission (350 nm)	0°	PMT	Xenon flash lamp	AU	96-well plate	200 µl	0 – 100	0.982
	Light transmission (600 nm)							0 – 100	0.983
Dual DLS/SLS plate reader (DynaPro III)	Light scattering	169°	Linearized avalanche photodiode detector	830 nm diode laser	TU	384-well plate	100 µl	0 – 60*	0.999
Visual inspection	Visual comparison	~15°	Naked eye	Diffuse daylight	NTU	2R glass vial	1 ml	Visual comparison to turbidity standards I-IV; (3, 6, 18 and 30 NTU)	n.a.

AU, absorbance unit; FNU, formazin nephelometric unit; LED, light-emitting diode; NTU, nephelometric turbidity unit; NTRU, nephelometric turbidity ratio unit; PMT, photomultiplier tube; TU, turbidity unit.
* calibrated with polymer standard and fitted with a quadratic function.

Table 2
Collection of biopharmaceutical products and samples. The Z-average hydrodynamic diameter and PDI values (%PD) were obtained by DLS measurements with respective samples that were employed in this study.

Sample	Description	Concentration during opalescence measurements	Hydrodynamic diameter determined by cumulant analysis (DLS) [nm]	%PD by cumulant analysis [%]
Aged epo	34-kDa protein	40,000 IE/ml	159.2 ± 21.9[(1)]	Multimodal[(1), (2)]
Aged abatacept	150-kDa protein	125 mg/ml	9.6 ± 0.1[(1)]	Multimodal[(1), (2)]
AAV	Non-enveloped virus	$2*10^{12}$ cp/ml	25.6 ± 0.6[(1)]	Multimodal[(1), (2)]
Sendai virus	Enveloped virus	6000 HA units/ml	200.0 ± 0.8	35.6
Liposomes	Lipid assembly	0.20 mg/ml	168.0 ± 0.1	11.8
PLGA nanoparticles	Model delivery system	0.18 mg/ml	125.6 ± 0.4	7.4
Alum adjuvant	Particulate adjuvant	0.05 mg/ml	780.4 ± 179.7[(1)]	Multimodal[(1), (2)]
Jurkat cells	Model T cell	$1*10^6$ cells/ml	Out of range[(1)]	Multimodal[(1), (2)]
Polymer-based standard suspension	Turbidity calibration standard	10 NTU	191.4	9.3

[(1)]Results from the cumulant analysis are shown for reference as they represent sufficiently well the size of the main particle population (i.e., estimated by the Dynamics software as greater than 95 % in average of the total mass content). Nonetheless, the DLS autocorrelation function clearly showed the presence of multiple distributions. *The intensity distribution for each sample, calculated from the regularization analysis, can be found in Supplementary information Figure S3.*
[(2)]If the %PD cannot be accurately determined, the Dynamics software labels it as "Multimodal". From a theoretical point of view the maximum polydispersity for a truncated gaussian distribution is approximately 57 %.

final volume was added (followed by 1 h equilibration). Down-sizing of the obtained liposomes was done via extrusion with a Lipex extruder (Northern Lipids Inc., Canada), the particles were extruded four times through a 400-nm and four times through a 200-nm polycarbonate filter (Nucleopore Milipore, Kent, UK) and the final concentration of 0.2 mg/ml was adjusted with 10 mM sodium phosphate buffer at pH 7.4. The adeno-associated virus (AAV) sample contained $2 * 10^{12}$ cp/ml (determined by a calibrated size exclusion chromatography method) as previously described (Rieser et al., 2022). The sample, consisting largely of empty AAV8-pseudotyped AAV2 capsids, was separated by anion exchange chromatography from the capsids containing a self-complementary (sc) vector genome containing eGFP under the control of a cytomegalovirus (CMV) promoter. The AAV capsids were eluted from the column in 60 % buffer A: 10 mM Tris, 10 mM bistrispropan, 2 mM magnesium chloride, 0.1 % poloxamer 188, pH 8 and 40 % buffer B: 10 mM Tris, 10 mM bistrispropan, 2 mM magnesium chloride, 0.1 % poloxamer 188, pH 10 (Rieser et al., 2021). Sendai virus (Cantell strain) with hemagglutination (HA) tube titer of 1:6000 in allantoic fluid was purchased from Charles River and was filtered through 5-µm polyether sulfone syringe filter (Pall) before analysis. The human immortalized T lymphocyte cell line Jurkat (clone E6.1) was purchased from CLS cell line service (Eppelheim, Germany). The cells were cultured in 90 % Roswell Park Memorial Institute (RPMI) 1640 (Thermo Fisher Scientific) medium supplemented with 10 % fetal calf serum (FCS) (Bio&SELL GmbH) at a density between 0.5 and $3 * 10^6$ cells/ml. Cells were harvested by centrifugation at 200 rcf, resuspended in fresh RPMI medium and were subsequently stored frozen with 10 % (v/v) dimethyl sulfoxide at approx. –140 °C. Before being used for the study, cells were thawed at

37 °C in a water bath, washed in fresh RPMI medium and finally diluted to a concentration of 1 * 10^6 cells/ml. Alum adjuvant composed of colloidal-suspended aluminum hydroxide (G Biosciences catalog no. 786–1215) was purchased from VWR and was diluted in ultrapure water to a final concentration of 0.05 mg/ml. To get insight into the contribution of the formulation ingredients to the obtained opalescence values, background samples were prepared as described in Table S1.

2.2. Opalescence measurements

Table 1 provides an overview of the instruments, as well as instrument parameters used in this study.

2.2.1. Calibration of opalescence instruments

All involved instruments in this study were calibrated in the first place with commercially available and certified formazin standard suspensions suitable for calibration, with nominal opalescence of 0.335, 0.994, 3.14, 6.07, 10.28, 20.2, 30.6, 100.7 NTU (StablCal, Hach Lange). These suspensions represent dilutions of a 4000 NTU formazin stock suspension, manufactured by using a buffer to stabilize formazin that otherwise chemically deteriorates over time. Importantly, they share the same scattering behavior compared to traditional formazin dilutions that were prepared by using ultrapure water. Apart from a homogenization step that was performed according to the manufacturer's instruction, these suspensions are ready to use. Furthermore, the dynamic range of the instruments was tested upfront with a serial dilution of a certified, nominal 1005-NTU formazin standard (Supplementary Figure S1) to ensure that the measured opalescence values from the tested samples (<100 NTU) were within the linear range of each instrument (except from the dual DLS/SLS plate reader). To test the influence of different calibration standards that are suitable for calibration, commercially available standard suspensions of styrene divinylbenzene microspheres with nominal opalescence of 0.2, 1, 10.2, 20, 41, 62, 103.6, and 1036 NTU qualified for non-ratio nephelometers (Reagecon Diagnostics) were used. This standard consists of cross-linked styrene divinylbenzene copolymer that forms uniform spheres, formulated in an ultrapure and aqueous buffer. It is commonly characterized by a smaller and more narrow size distribution compared to formazin. The standard suspensions were used after a homogenization step that was performed according to the manufacturer's instructions. In all cases, the nominal (certified) opalescence values from the standards were used for instrument calibration. Suitable calibration curves were generated in the range between 0 and 100 NTU.

2.2.2. Ratio nephelometer

A Hach 2100AN turbidimeter (Hach Lange) operating at 400 – 600 nm (by using a USEPA filter) was used for opalescence measurements in the ratio mode. The instrument detects light primarily at 90°, as well as at 30° (forward scattering) and 0° (transmission signal) to correct for artefacts due to sample coloration. Backscattering at 138° is measured in case of high opalescence above 4000 NTRU. For each measurement, 2.0 ml of sample were analyzed.

2.2.3. Non-ratio nephelometer

A NEPHLA nephelometer (Hach Lange), operating at 860 nm and detecting at a 90° angle, was used for non-ratio nephelometric opalescence measurements. For the measurement, 2.0 ml of each sample were analyzed.

2.2.4. Microplate nephelometer

A NEPHELOstar Plus instrument (BMG Labtech) equipped with a clear 96-well plate (Greiner Bio One) was used for the nephelometric measurements. The reader detects forward scattering within an angle of 0 – 80° by collecting scattered light with an Ulbricht sphere and uses laser light at 635 nm. All samples were analyzed in triplicates using 200 µl sample per well. The laser intensity was set to 60 % and the beam focus to 2 nm.

2.2.5. Absorbance plate reader

A Synergy Neo2 multi-mode plate reader (BioTek) was used for the turbidimetric measurements. 200 µl of each sample were added in triplicate to clear-bottom 96-well plates (Greiner Bio One). Turbidimetry (transmission signal at 0° scattering angle) was measured at 350 nm and 600 nm by using the reader's end point configuration and by using the Gen5 software for data evaluation. Pathlength correction was performed by using the wavelengths of 900 and 998 nm, as well as a correction factor of 0.15104. The absorbance of an empty well was subtracted as blank.

2.2.6. Dual DLS/SLS plate reader

A DynaPro Plate Reader III instrument (Wyatt Technology) was used to implement opalescence measurements in a high-throughput format by exploiting its capability to measure static light scattering at an angle of 169° with a laser wavelength of 830 nm. Three wells per sample in a 384-well plate with a glass bottom (Wyatt) sealed by adhesive film (ThermoFisher) were used, with a sample volume of 100 µl per well. The plates were centrifuged for 2 min at 300 rpm before being placed in the plate reader. A laser intensity of 2 % was employed at an attenuation level of 0 % for opalescence measurements. One acquisition of 5 s was recorded per well.

Furthermore, the same instrument was used to characterize samples by DLS for which auto-attenuation was employed. Every measurement was performed with 10 acquisitions of 5 s. Three wells per sample were measured in an unsealed 384-well plate (Aurora) filled with 35 µl of sample. Data were collected and processed with the DYNAMICS software version 7.10 (Wyatt Technology). The coefficient of self-diffusion (D) and the polydispersity were calculated from the obtained autocorrelation functions by using cumulant analysis. The Stokes – Einstein equation was used to calculate the hydrodynamic diameter from D. Regularization analysis was used instead of the cumulant one, whenever appropriate by using standard DYNAMICS setting for the regularizer for optimum resolution and robustness of the calculation. Liposomes and alum adjuvant were further diluted to 0.02 mg/ml and 0.01 mg/ml, respectively.

2.3. Clarity and degree of opalescence

Clarity and degree of opalescence were assessed according to Ph. Eur. 2.9.20. To do so, the samples were manually filled into 2R glass vials (Schott, Fiolax Clear, Clear Line), which were closed with Fluorotec injection stoppers (West) and crimp-capped (West). The analyses were performed independently by two trained examiners.

2.4. Color

Sample coloration was measured with a spectral colorimeter (LICO 690 Professional, Hach Lange) in accordance with Ph. Eur. 2.2.2. For this, a sample volume of 500 µl was employed in transparent disposable cuvettes.

3. Results

3.1. Molecular size, color, visual appearance, and opalescence of employed samples

In a first step all biopharmaceutical samples involved in the study were characterized by DLS. A broad range of apparent molecular sizes and size distributions was covered by the selected sample set (Table 2), ranging from a hydrodynamic diameter of ~ 10 nm to 780 nm for the aged abatacept and alum adjuvant, respectively, whereas the theoretical diameter of the Jurkat cells lied above the upper size limit of the DLS instrument. Relatively monodisperse size distributions were obtained

for liposomes and PLGA nanoparticles, indicated by a percental polydispersity below 12 %, in contrast to highly polydisperse representatives like the aged epo protein, which resembled a typical sample from an accelerated stress study.

Furthermore, color, clarity and the degree of opalescence were assessed according to the procedures defined in the Ph. Eur. (Table 3). As sample coloration can interfere with certain opalescence measurements, it was assessed for the sample set, identifying aged epo and AAV samples as entirely colorless. A slightly brown color (B3) was detected for the Sendai virus, a red color for the Jurkat cells (R4), a moderate brown color for liposomes, PLGA nanoparticles and alum adjuvant (each B6) and a relatively strong brownish-yellow color for the abatacept sample. Furthermore, the assessment of clarity and degree of opalescence showed that aged epo, aged abatacept and AAV samples had a clear appearance (<I), whereas the opalescence gradually increased via the PLGA nanoparticles, liposomes, and alum adjuvant to the highest opalescence detected by the naked eye in the Sendai virus sample (>IV).

To instrumentally assess the opalescence of all samples, a frequently employed ratio nephelometer calibrated with stabilized formazin calibration suspensions was used in the first step (Fig. 1). Importantly, to ease the comparison with opalescence results obtained from subsequently employed instruments, all values are stated in the most general way by using turbidity units (TU) in the following. For clarification, the appropriate technical unit for each instrument is presented in Table 1. The detected opalescence values from the ratio nephelometer were ranging from close to zero up to 71.2 TU (Fig. 1) and corresponded decently well to the results obtained from the visual method in Table 3 according to Ph. Eur. 2.2.1. Only liposomes, PLGA nanoparticles and alum adjuvant were rated with a lower opalescence by the naked eye when compared to the results of the ratio nephelometer.

Notably, the polarizability of each sample, its particle concentration, and particle size distribution (including particulate impurities and degradation products) are expected to strongly affect the respective light scattering properties. However, these parameters differed to a large extent in the various samples (Table 2). Therefore, unambiguously allocating the observed differences in opalescence values to a single property of the samples remains difficult. Nevertheless, samples with a diameter in the low nm-size range like abatacept (~10 nm), as well as the AAV (~25 nm) yielded values clearly below 10 TU. In contrast, samples in the sub-micron size range with particles larger than 100 nm like liposomes, PLGA nanoparticles and alum adjuvant, yielded in values clearly above 30 TU. As shown in Table S1, opalescence measurements of the background, i.e., formulation components without the “active” pharmaceutical ingredient suggest that the observed opalescence predominately originates from the “active” pharmaceutical ingredient. In summary, the performed analyses demonstrated the diversity and heterogeneity of the employed sample set, making it representative for many biopharmaceutical applications.

Table 3
Degree of coloration, clarity and degree of opalescence according to the procedures defined in the Ph. Eur. The letters B, BY and R indicate the colors brown (B), brownish-yellow (BY) and red (R), respectively, and high numbers indicate a strong coloration. Clarity and the degree of opalescence were determined by two examiners that came to equal results. Roman numerals refer to the formazin reference suspensions 3 NTU (reference suspension I), 6 NTU (reference suspension II), 18 NTU (reference suspension III) and 30 NTU (reference suspension IV).

Sample	Degree of coloration Ph. Eur. 2.2.2	Clarity and degree of opalescence Ph. Eur. 2.2.1
Aged epo	Colorless	< I
Aged abatacept	BY7	< I
AAV	Colorless	< I
Sendai virus	B3	> IV
Liposomes	B6	III < … < IV
PLGA nanoparticles	B6	II < … < III
Alum adjuvant	B6	III < … < IV
Jurkat cells	R4	Interference due to coloration

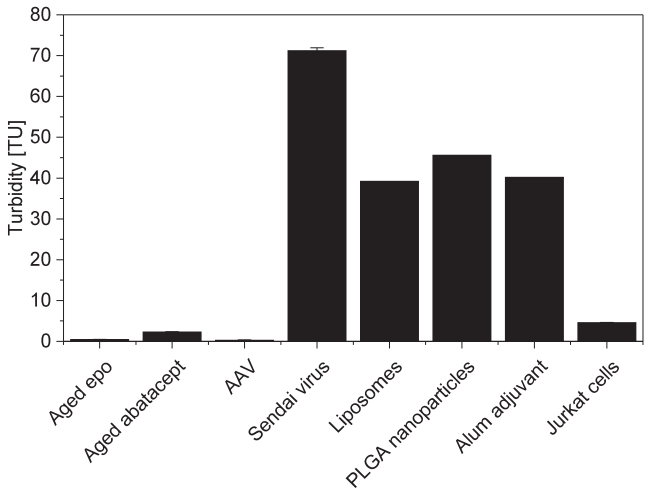

Fig. 1. Opalescence of various biopharmaceutical samples determined with a ratio nephelometer which was calibrated with formazin standard suspensions. For comparison, results of the opalescence measurements are presented as turbidity units (TU) while acknowledging that the employed instrument yields opalescence values in NTRU as the technical unit (see Table 1). Error bars refer to triplicate measurements. Single measurements were performed in case of Liposomes, PLGA nanoparticles and Alum adjuvant.

3.2. Comparison of opalescence measurements between different instruments

Opalescence measurements were compared between various commonly used instruments, a non-ratio nephelometer, a microplate nephelometer and an absorbance plate reader at 350 nm and 600 nm in addition to the ratio nephelometer that was used in the previous section (Table 1). Since the visual method according to Ph. Eur. 2.2.1 yields semi-quantitative ranges of opalescence only, the results of this method were excluded from the instrument comparison. Importantly, despite all instruments had been calibrated with the same stabilized formazin standard suspensions, very large discrepancies were observed among the various instruments and measurement principles as it is illustrated in Fig. 2. Remarkably strong deviations between methods were further indicated by very high relative standard deviations observed for each sample (Supplementary Table S2 together with the tabulated opalescence data of Fig. 2).

To better reveal systematic differences between the instruments, radar plots are shown for each sample in Fig. 3. First, the absorbance plate reader yielded substantially increased opalescence values at 350 nm for the aged abatacept and the Sendai virus, as well as at 350 nm and 600 nm for the Jurkat cells. Importantly, absorbance spectra were measured for each sample (Supplementary Figure S2). They indicated a substantial contribution from light-absorbing formulation components in the case of the Sendai virus at 350 nm and to some extent of the Jurkat cells at 350 nm and 600 nm. Measurements performed on the background samples confirmed that part of the observed absorbance originates from the media of both materials (Table S1). Such absorbance adds to the reduced light transmission from light scattering and leads to overestimated opalescence. This effect was much less pronounced in the aged abatacept sample, as the elevated signal in the 330 – 430 nm wavelength range could not be unambiguously assigned to absorbance or light scattering. Therefore, the presence of absorbing formulation compounds explained at least partly the increased opalescence obtained from the absorbance plate reader in Sendai virus and Jurkat cell samples and potentially in the aged abatacept sample. The differences among the instruments were particularly strong for the aged abatacept sample,

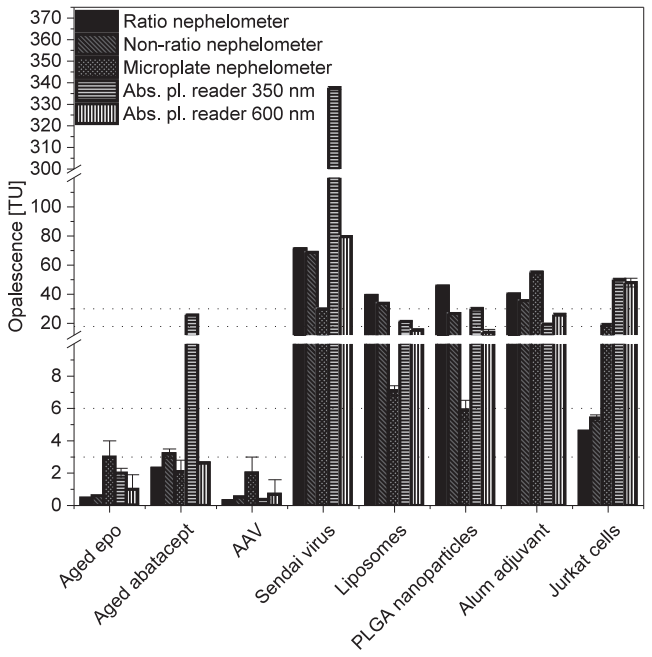

Fig. 2. Opalescence measurements of various biopharmaceutical samples with a set of different methods and instruments. Instruments were calibrated with formazin standard suspensions. For comparison, results of the opalescence measurements are presented as turbidity units (TU) while acknowledging that each instrument provides a different technical unit (see Table 1). Error bars refer to triplicate measurements. For Liposomes, PLGA nanoparticles and Alum adjuvant, single measurements were performed with the ratio nephelometer and the non-ratio nephelometer, respectively. Dotted lines mark Ph. Eur. reference suspension I (3 NTU), II (6 NTU), III (18 NTU), and IV (30 NTU).

differing by a factor of twelve between the microplate nephelometer (2.1 TU) and turbidimetry at 350 nm (25.8 TU).

Second, for aged epo, AAV and alum adjuvant samples, the microplate nephelometer yielded higher opalescence values as compared to the ratio nephelometer. The reason for these increased levels is less obvious and might be based on sample coloration in case of alum adjuvant compared to the colorless aged epo and AAV samples (see Table 3) and on the combination of particle size and the detection of the forward scattering signal in the microplate nephelometer (see discussion section). Finally, even between the nephelometers with the seemingly most similar optical properties (ratio and non-ratio nephelometers), substantial differences were observed, for example in the aged abatacept, AAV, and PLGA nanoparticle samples. Therefore, the performed instrumental analyses clearly demonstrated large discrepancies between the methods despite a calibration step with formazin standard suspensions applied for all instruments. This illustrates that opalescence measurements are relative methods within the respective instrument settings, an aspect which is fundamental but frequently disregarded in the field and further explicated in the discussion section.

3.3. Comparison of formazin and polymer-based calibrations

The observation of large discrepancies in the context of formazin-calibrated instruments led to the question of how an alternative polymer-based calibration standard would affect opalescence measurements of the same samples. Standard suspensions of styrene divinylbenzene microspheres were previously used in the biopharmaceutical field, for example to characterize the opalescence of monoclonal antibodies (Kingsbury, 2020). In fact, alternative standards can represent another source for the lack of inter-laboratory comparability of opalescence measurements. To demonstrate this, all instruments previously calibrated with formazin were re-calibrated with standard suspensions of styrene divinylbenzene microspheres, which were certified for non-ratio nephelometers (Fig. 3). Notably, absorbance spectra for formazin and polymer-based standard suspensions did not show contributions from an absorbing species at the wavelengths 350 nm and 600 nm (see Supplementary Fig. S2I and J, respectively).

Presumably, the usage of certified polymer standard suspensions with a well-defined value intuitively suggests obtaining opalescence values for each sample that are equal to those using the formazin calibration. However, this is only observed for the non-ratio nephelometer (Fig. 3), for which the polymer-based standard was certified and for which opalescence values from both calibrations nicely overlap in most samples. In all remaining instruments, substantial differences were obtained between the two calibrations, which were particularly strong for the microplate nephelometer and to some extent for the absorbance plate reader. The observed differences are due to the differences in the calibration curves of both standards for each instrument (Fig. 4).

Formazin and polymer-based calibration curves overlapped fairly well in the non-ratio nephelometer, as expected from the certification of the polymer-based standard for non-ratio nephelometers. In contrast, moderate deviations occurred in the ratio nephelometer and the absorbance plate reader, whereas substantially different calibration curves were obtained in the microplate nephelometer. In the latter, much higher opalescence values are obtained from the same raw signals if the microplate nephelometer was calibrated with the polymer standard instead of formazin. The presented calibration curves confirm that the use of alternative opalescence standards might introduce an additional source of a poor inter-laboratory comparability of opalescence measurements.

3.4. High-throughput opalescence measurements with a dual DLS/SLS plate reader

Commonly used nephelometers come with the drawback of requiring high sample volumes (up to 2 ml) and a lack of temperature control. Other microplate nephelometers or absorbance plate readers can deviate substantially from large volume nephelometry measurements as shown in the previous sections. Therefore, we investigated the possibility to measure opalescence in a 384-well format by exploiting a dual DLS/SLS plate reader, which would be highly beneficial for formulation development and developability assessments. Under temperature-controlled conditions, it would allow combining the low volume turbidity readout with the additional molecular characteristics of hydrodynamic diameter and molecular weight. These are highly useful parameters that can be used to assess samples at various stages of the development of biologics.

With an 830-nm laser, the reader emits light in the infrared region and detects the light scattering signal at an angle of 169° (backscattering). This detection angle makes the developed method substantially different from classical nephelometry or turbidimetry. Interestingly, an attempt to calibrate the dual DLS/SLS plate reader with formazin standard suspensions yielded extremely noisy and incoherent signals (Fig. 5A), an observation that was independent of instrument settings like the employed laser intensity (data not shown). In contrast, the polymer-based alternative standard for non-ratio nephelometers between 0 and 60 NTU yielded a coherent calibration curve of decent quality. However, a non-linear relationship between nominal opalescence and resulting raw signal was observed (Fig. 5B). Fig. 5C shows normalized calibration curves of the polymer standard for increasing laser power, demonstrating that the non-linear behavior appears to be independent from the employed laser intensity.

However, to investigate its potential value by obtaining an approximate ranking of different samples based on their opalescence, calibration curves were fitted with a quadratic function and all involved biopharmaceutical samples were characterized with the proposed high-throughput opalescence method at 25 °C. Subsequently, the obtained values were compared with the results from the previously employed

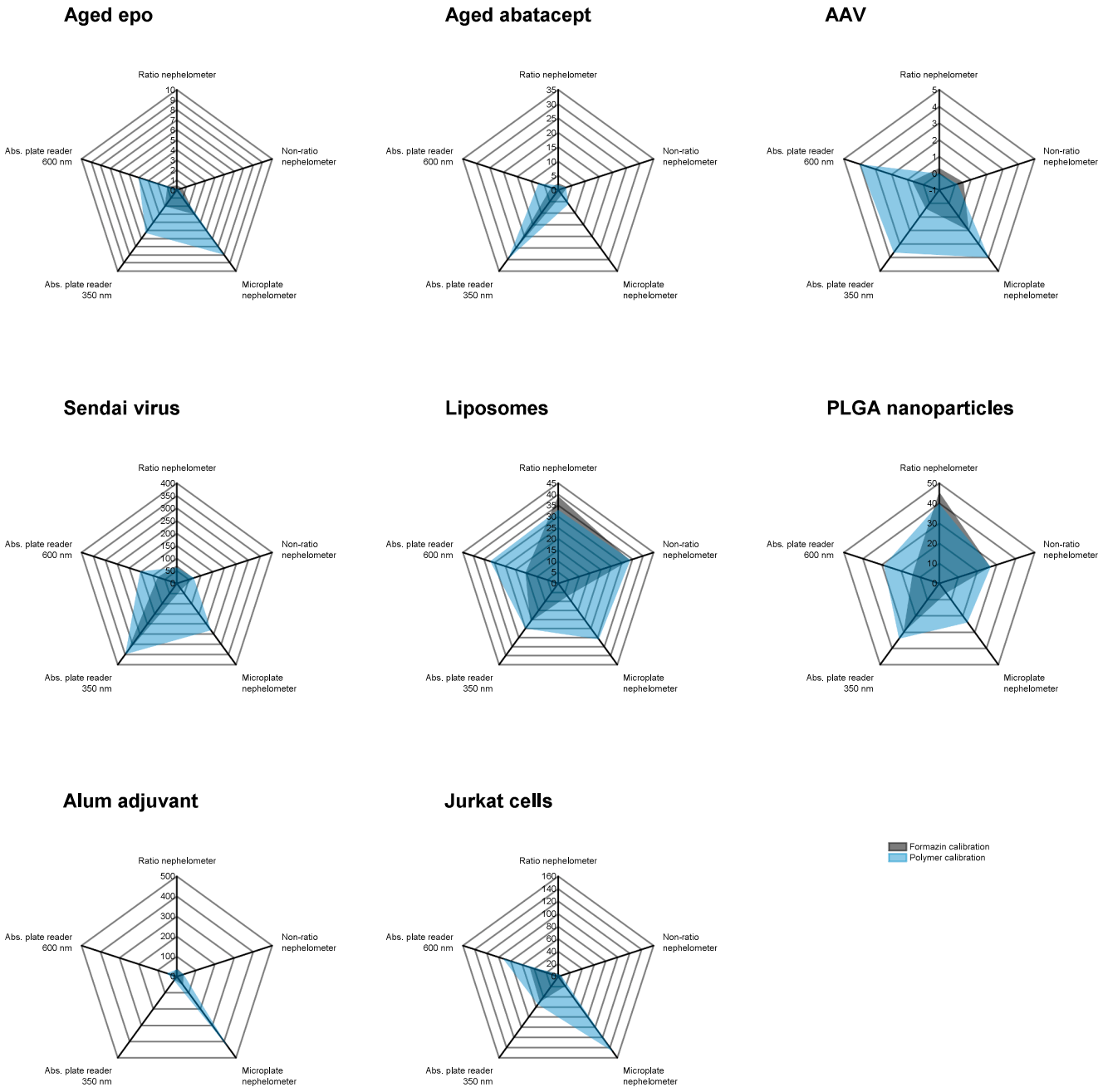

Fig. 3. Comparison of opalescence measurements after calibrations with formazin (grey area) versus styrene divinylbenzene microsphere standards (light blue area). (For interpretation of the references to color in this figure legend, the reader is referred to the web version of this article.)

instruments upon calibration with polymer-based standard (Fig. 6). Interestingly, the dual DLS/SLS plate reader yielded opalescence values for all samples that were in the same range as the results of the ratio and non-ratio nephelometers, except from the alum adjuvant sample (Fig. 6 and Supplementary Table S2). This was in strong contrast to the substantial deviations previously observed for the absorbance plate reader and microplate nephelometer when they were compared to the ratio and non-ratio nephelometers. This suggests that the obtained opalescence values from the dual DLS/SLS plate reader are closer to the ones obtained by nephelometry according to Ph. Eur. Consequently, this novel method extends the applications of a dual DLS/SLS plate reader beyond molecular weight, size and protein interaction determination (Gentiluomo et al., 2020) by offering an opalescence ranking that can be useful in the early development stage of biologics. Laboratories that are already using a dual DLS/SLS plate reader during product development can benefit from additional opalescence analysis without extra standalone instruments.

4. Discussion

Beyond quality control testing using compendial methods (e.g., Ph. Eur 2.2.1), opalescence measurements find broad application in the development of biopharmaceuticals and ATMPs. For instance, opalescence is a fast readout during upstream processing to characterize the clarity of cell culture broth. Opalescence values of 4–14 NTU and 430–540 NTU were measured post bioreactor for lentivirus in adherent HEK293T cell process and AAV in lysed HEK293 cell suspension process, respectively (Raghavan et al., 2019). Similarly, other authors reported opalescence values of lentivirus-containing cell suspensions of 141 NTU for 1.1 x10^6 cells/ml and 382 NTU for 3.7 $\times$ 10^6 cells/ml before

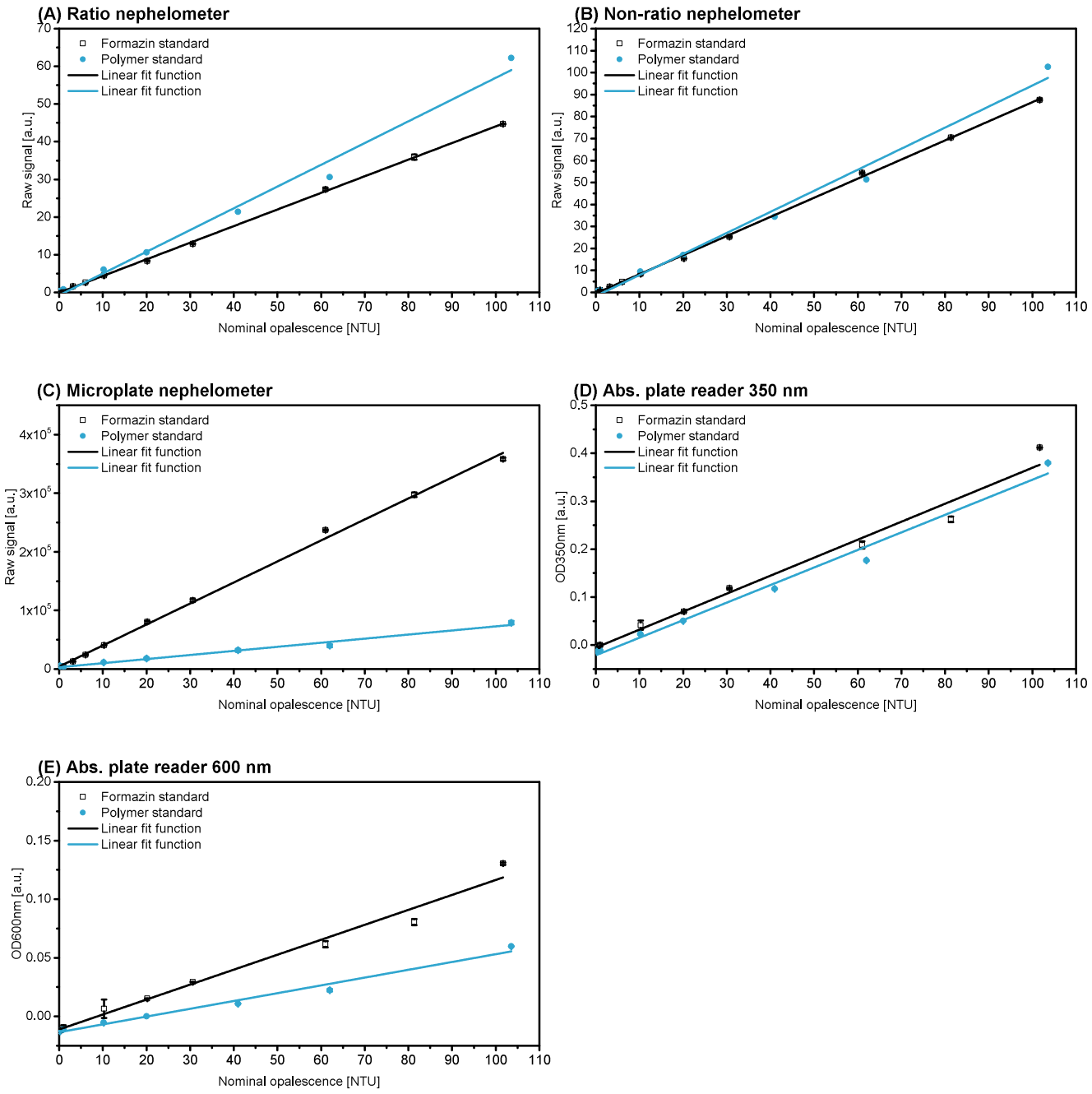

Fig. 4. Calibration curves obtained for formazin standards and polymer standards (styrene divinylbenzene microspheres). Error bars refer to triplicate measurements. Single measurements were performed with the polymer standards in case of the ratio and non-ratio nephelometer.

clarification (Labisch et al., 2021). These reports indicate that a broad range of low and high opalescence can be encountered depending on the cell culture process, as well as cell concentration before clarification of the harvest. Even after clarification, the opalescence of lentivirus solution ranged between 18 and 43 NTU, depending on which procedure was used (Labisch et al., 2021).

Similarly, opalescence measurements play an important role in formulation development, developability assessment and CMC strategies of biopharmaceutical proteins, because they are a critical quality attribute and an early indicator of "not well-behaving" candidates for complex and diverse reasons including presence of irreversible aggregates, reversible associates, or liquid–liquid phase separation. The underlying mechanisms and implications of opalescence and related liquid–liquid phase separation of proteins are excellently reviewed by Raut and Kalonia (Raut and Kalonia, 2016). Interestingly, Kingsbury *et al.* found k_D measurements at low, as well as high ionic strength to be indicative for solution viscosity and opalescence of mAbs, although both properties themselves were remarkably unrelated (Kingsbury, 2020). Interestingly, the same study gave a broader perspective on typical opalescence values. Kingsbury *et al.* measured opalescence values below 12 NTU for 51 out of 59 mAbs at 150 mg/ml in 10 mM histidine buffer at pH 6 and found 8 mAbs that were more opalescent (comprising no IgG1, 1 out of 4 tested IgG2 and 7 out of the 11 tested IgG4) (Kingsbury, 2020).

To measure opalescence, a calibration step with formazin is commonly assumed to allow a direct comparison of opalescence measurements in the biopharmaceutical literature, even if the data was generated with different instrument settings. In fact, instrument calibration with formazin or any other turbidity standard can lead to a

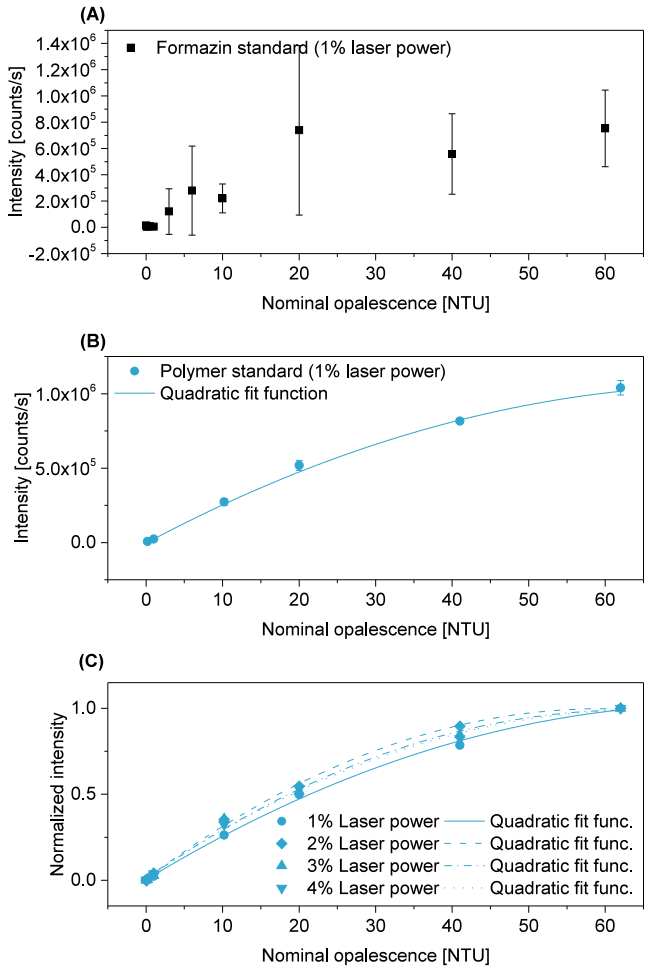

Fig. 5. Comparison of exemplary calibration curves for formazin (A) and polymer (B) standards by using the static light scattering functionality of a dual DLS/SLS plate reader at 1 % laser power. A quadratic function was fit to the data points in case of polymer standard (B). Normalized intensities obtained with polymer standards at various laser powers (C). Measurements were performed at 25 °C. Error bars in (A) and (B) refer to the measurements of 3 wells per sample.

misleading sense of comparability and tends to obscure the fact that absolute comparisons of opalescence values are very challenging to achieve. The observed discrepancies between the tested instruments in this study illustrate that this might be one of the main misunderstandings in the biopharmaceutical field, contributing to poor inter-laboratory comparability of opalescence measurements, as pointed out by Barros and colleagues (Barros et al., 2021). The fact that a calibration step with formazin does not necessarily lead to equal results from different instruments can have three major reasons.

First, some of the tested samples in our study like Sendai virus, liposomes, PLGA nanoparticles, Alum and Jurkat cells showed a certain degree of coloration, which is further supported by the respective absorbance spectra of Sendai virus and Jurkat cells, hinting towards absorbing formulation components. Sample coloration might bias the measurements in instruments with a resonating wavelength range. Notably, by employing light in the infrared region, the non-ratio nephelometer and the dual DLS/SLS reader are expected to be unaffected by the observed sample coloration. Furthermore, the ratio nephelometer used in this study can correct for coloration effects in the ratio mode. Therefore, these instruments offer the most robust measurements in case of colored samples.

Second, a combination of intrinsic and extrinsic factors and their interactions affects the light intensity that is monitored by a light scattering detector. The refractive index of each sample, its particle concentration and particle size distribution (including particulate impurities and degradation products) strongly affect the scattering intensity and its angular dependence. The angular dependence can be addressed in two ways: (i) Particles smaller than the wavelength of incident light obey Rayleigh scattering theory which predicts an isotropic angular distribution of the scattered light. (ii) Particles larger or close to the wavelength of incident light obey Mie scattering theory which predicts an anisotropic angular distribution of the scattered light. Importantly, such theories assume single scattering where the total scattered field is assumed to be the sum of all fields scattered by individual particles, each of which is excited by the external field in isolation from other particles. However, multiple scattering is expected for turbid samples and an analysis based on the stated theories is not applicable in this case. Interestingly, the effect of multiple scattering is known to be of special concern for large particles with high refractive index, such as in the case of the formazin standard. This would in principle limit an accurate signal interpretation based on the Mie theory only for very low concentrations.

Finally, differences in the optical properties of instruments are commonly expected to be compensated by the calibration step, i.e., making the opalescence values obtained at two different detection angles comparable. However, this can only be achieved if the employed calibration standard perfectly resembles the investigated sample with respect to particle size, shape and polarizability, leading to identical optical properties between sample and standard.

It is well illustrated by aged epo and AAV that a direct comparison of opalescence measurements is not straightforward: aged epo and AAV samples were characterized as colorless (Table 3), but they showed instrument-dependent differences in absence of a potential color bias (Fig. 2). For both samples, the microplate nephelometer, which integrates the forward scattering between 0° and 80°, yielded substantially higher values compared to the ratio and non-ratio nephelometers (Fig. 2), which themselves showed differing opalescence values. Finally, the opalescence values obtained from the absorbance plate reader at both wavelengths lay between the values obtained from the nephelometers, complementing the picture of arbitrary opalescence results in different instruments even in absence of a color-induced bias.

The central role of the calibration standard formazin and its original field of application is particularly interesting from a biopharmaceutical perspective. Historically, the search for an opalescence standard mainly happened in the context of water quality testing to investigate sediment-containing samples with a broad distribution of shapes and sizes (Sadar). Formazin standard suspensions were previously shown to have a hydrodynamic diameter of 946 nm with a broad size distribution (%PD = 26.8) (Barros et al., 2021), thereby reflecting the required properties as an opalescence standard for aforementioned samples (Sadar). In strong contrast, many biopharmaceutical products are found in a completely different regime of particle size and are aspired to be highly monodisperse, at least in the unstressed state. Consequently, they are expected to have largely different optical properties compared to formazin. Indeed, the latter strongly scatters light of ca. 660 nm at 0° (forward scattering), but only weakly at 180° (backward scattering), as it is the case for a classical Mie scatterer (Barros et al., 2021). In strong contrast, the angular dependence of the scattered light from a (highly monodisperse) mAb was shown to be almost zero (Barros et al., 2021). Furthermore, the formazin standard is expected to be prone to multiple scattering due to its high refractive index and particle size. Consequently, measurements of one and the same biopharmaceutical sample in formazin-calibrated instruments with different detection settings, can result in tremendously different opalescence values. Particularly the results in Fig. 2 of our study underline this problem and demonstrate it for a broad set of biopharmaceutical samples. They further illustrate that opalescence measurements should be understood as a relative readout that needs to be considered within the framework of the respective instrument settings that were applied for data collection.

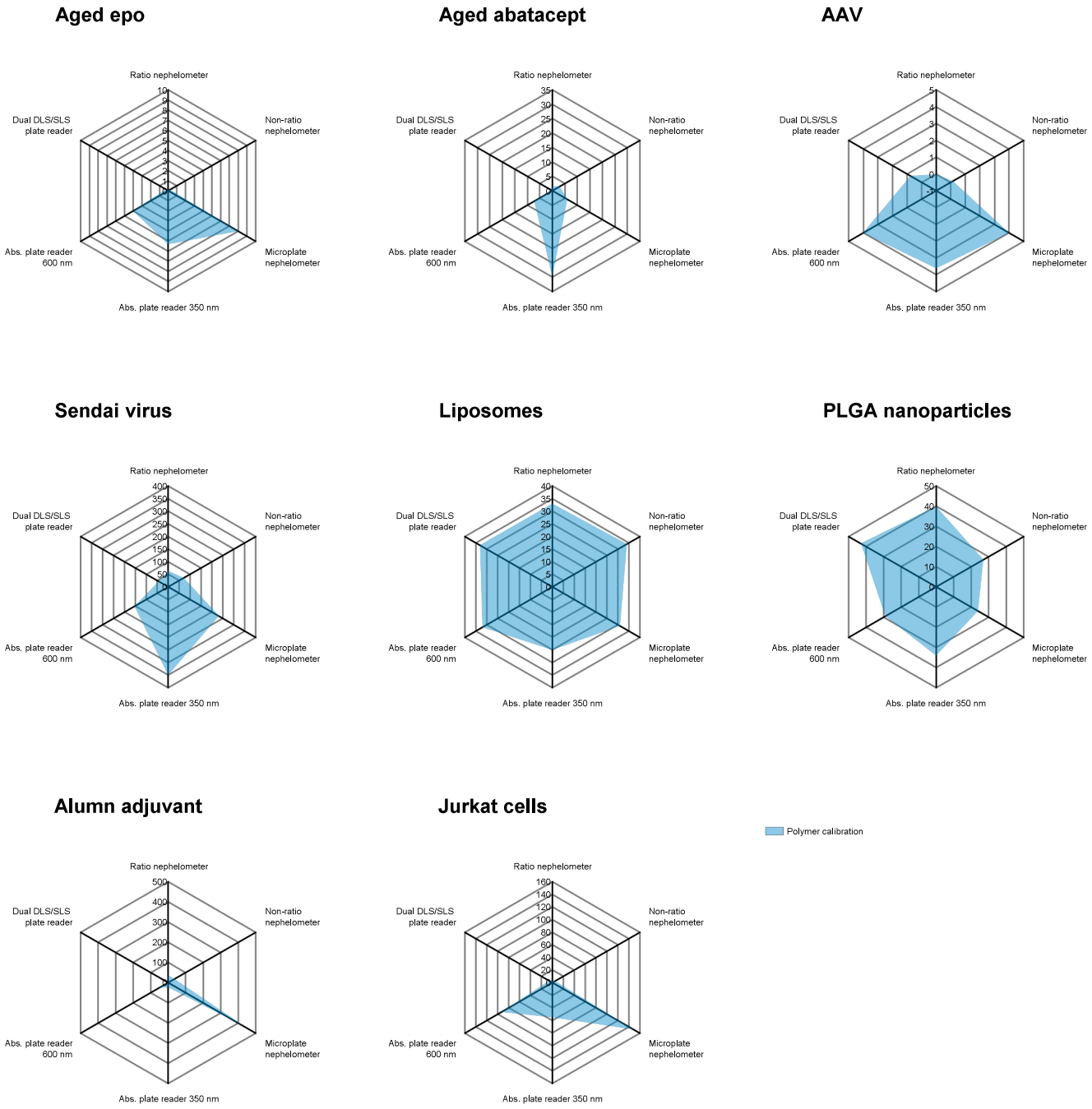

Fig. 6. Opalescence of diverse biopharmaceutical samples measured with a dual DLS/SLS plate reader in a 384-well format at 25 °C, in comparison with the remaining instruments for opalescence measurements. All instruments were calibrated with a polymer-based opalescence standard.

As formazin presents evident challenges for inter-laboratory comparability we investigated an additional calibration standard: As shown in Fig. 3, the use of such a standard resulted in dramatically different responses in the microplate nephelometer compared to its formazin counterpart. As a result, extremely different opalescence values were obtained between both calibrations, particularly for turbid samples (Fig. 3). It is important to realize that polymer-based opalescence standards share a substantially different distribution of particle size and shape compared to formazin as well as a different refractive index. Based on DLS, the polymer standard used in this study was characterized by an average hydrodynamic diameter of 191 nm and a monodisperse distribution (%PD = 9.3), which is substantially lower compared to the hydrodynamic diameter of 946 nm of formazin and its broad distribution (%PD = 26.8) (Barros et al., 2021). Importantly, polymer standards are designed to mimic the response obtained from the corresponding formazin standard only for a single and well-defined instrument setting, usually for ratio or non-ratio nephelometers. This can be seen very well in Fig. 4, where the response curves of formazin and non-ratio polymer standard nicely overlap only in case of the non-ratio nephelometer. In strong contrast, the substantially different scattering angle of 0° – 80° and a laser wavelength of 635 nm led to the strong discrepancy between formazin and polymer standard in the microplate nephelometer since both standards behave fundamentally different under those scattering conditions.

Another challenge of opalescence measurements for biopharmaceutical samples can be the high sample volume needed for classical, Ph. Eur. compliant instruments. However, the transition from a nephelometer instrument with a well-defined optical path into a plate reader

format is a technical challenge. The well-design of the plate largely prevents a nephelometric detection mode at a scattering angle of 90°, making the resulting opalescence values incomparable to classical nephelometers. Although turbidimetry can be conveniently applied in a plate-based format by using absorbance readers, it has the disadvantage of potential interference with sample absorbance (color) and is less sensitive compared to nephelometry, particularly if high wavelengths are employed. This can be seen by the relatively small absorbance values obtained at both wavelengths in Fig. 4, illustrating the reduced sensitivity of plate-based turbidimetry in comparison to the remaining methods.

Nevertheless, high-throughput opalescence measurements can be highly beneficial at diverse stages of the development process of biologics. Therefore, three methods applicable in high-throughput scale were included and developed in our study. Besides the absorbance plate reader and a commercially available microplate nephelometer which integrates the forward scattering signal up to an angle of 80°, we investigated the use of a dual DLS/SLS plate reader for nephelometric opalescence measurements by exploiting its static light scattering detection at a 169° angle. Importantly, a non-linear relationship of polymer-based calibration curves represents a limitation of the method, as it prevents accurate quantification of sample opalescence. Nevertheless, for most of the tested samples it yielded opalescence values that were in the range of those obtained from nephelometers complying with Ph. Eur. Therefore, the method can be used to rank samples based on their approximate opalescence, which can be highly useful as a developability assessment during early development stages or as a formulation screening and might be better suited for weakly opalescent samples than the use of an absorbance plate reader. Furthermore, a dual DLS/SLS microplate reader is often used for fast assessment of polydispersity, offering additional molecular information like molecular size and weight. Therefore, the developed method allows performing approximate opalescence measurements in a high-throughput format without the need for further instrumentation.

Notably, the reason for the non-linear behavior observed in the dual DLS/SLS plate reader remains unclear. A similar approach by using a cuvette-based SLS instrument was recently applied to measure the opalescence of monoclonal antibodies (Barros et al., 2021; Kingsbury, 2020), which lacks the possibility of high-throughput applications but provides a linear range of 0–200 NTU. This might suggest that the linearized avalanche photodiode detector in the dual DLS/SLS plate reader could play a role in the observed non-linearity. Furthermore, the dual DLS/SLS plate reader could only be calibrated with polymer-based standard suspensions. In contrast, calibrating with formazin resulted in large errors among replicates, preventing an unambiguous correlation between the nominal opalescence of the formazin standards and their corresponding raw signals (Fig. 5A). Several reasons exist that might explain this observation. Formazin has a hydrodynamic radius that is close to the upper size limit of the reader's DLS functionality (1000 nm), which might also complicate SLS measurements in this size region. Furthermore, the previously described phenomenon of multiple scattering is expected to be particularly strong in case of formazin, likely contributing to the large artefacts in the dual DLS/SLS plate reader.

Another remarkable observation was that the alum adjuvant gave rise to very low opalescence values in the dual DLS/SLS plate reader. With an average particle diameter of 780 nm (Table 2), its size lies in the range of the dual DLS/SLS plate reader's wavelength (830 nm), possibly reflecting the very low backscattering signal of a Mie scatterer. In strong contrast, the alum adjuvant was characterized as a highly opalescent sample in the microplate nephelometer (Fig. 6). The latter collects the forward scattering signal and employs a wavelength of 635 nm, suggesting that the strongly enhanced forward scattering of a Mie scatterer was detected in this case. Finally, this relationship is the most plausible explanation of strongly increased opalescence values in the microplate nephelometer upon calibration with the polymer-based standard (Fig. 3 and Fig. 4). With a smaller average particle size of 191 nm, the polymer-based standard is expected to represent a Rayleigh scatterer with more evenly distributed forward and backscattering signals and to be less prone to multiple scattering. If the instrument would be calibrated with the polymer-based standard, a sample with a strong forward scattering intensity may be characterized with a higher opalescence in comparison to the formazin-calibrated system, which accommodated the strong forward scattering of the formazin itself.

5. Recommendations and conclusions

Results from opalescence measurements of biopharmaceutical samples strongly depend on the used measurement principle (scattered light, reduced light transmission, etc.), the optical properties of the instrument (angle of detection, light source and respective wavelength or wavelength range, etc.), as well as on the interactions of the reference standards with light. In general, speaking of opalescence measurements instead of turbidity measurements appears more convenient, which includes both nephelometric and turbidimetric measurement principles. Moreover, although the unit of TU was used in this work to compare the different instruments, it is recommended to generally use the correct technical unit as outlined in Table 1, since each respective unit provides some information about the applied measurement mode.

Notably, the choice of the respective opalescence method and instrument setting should depend on the intended application, commonly ranging from early-stage characterization (screenings, low volume, high-throughput) to late-stage development activities and quality control testing with compendial methods. Based on our characterization of a broad set of biopharmaceutical samples with a set of different instruments, Table 4 gives an overview of instrument and method characteristics that should be considered for choosing the best-suited opalescence method for the respective application and lab setting. Furthermore, formazin as a calibration standard is characterized by a relatively large average diameter. Therefore, the use of polymer-based calibration standards with a smaller particle size might be more useful when characterizing samples in the size range of proteins and low nm-sized particles such as AAV. These standards are expected to better resemble the sample's optical properties, which would lead to less pronounced differences between different instruments. The following general recommendations can be made for opalescence measurements in a biopharmaceutical context:

Low-volume, high-throughput, and plate reader-based measurements are suitable for early-stage characterizations, where a relative assessment of the same product is sufficient to identify more turbid, i.e., often less promising candidates. Furthermore, due to the relative assessment of opalescence that might not comply with the Pharmacopoeia, the choice of the calibration standard might be less impactful. Both optical density (OD) measurements and microplate nephelometers are useful; however, OD measurements are commonly less sensitive compared to nephelometric approaches. Furthermore, readers that detect forward scattering signals are expected to be much more sensitive to large particles compared to readers that measure backscattering. This should be considered in the context of the respective sample that is to be analyzed. For early-stage high-throughput screenings, the presented novel approach by using a dual DLS/SLS plate reader with results more similar to a ratio nephelometer is particularly helpful, because it offers additional molecular information like molecular size and weight which can be highly beneficial for the development process of biologics and their formulations.

In contrast, compendial nephelometry according to the Pharmacopeia should be applied during late-stage development and quality control. There, high sample volumes are usually less of a problem and a calibration with formazin is required. Alternatively, a polymer-based standard, which is explicitly qualified for the respective instrument, can be used. Furthermore, ratio nephelometers offer robust opalescence measurements as the ratio mode can correct for artefacts that originate from sample coloration, at the same time offering a higher dynamic

Table 4
Overview of applications, recommended methods and their characteristics based on the instruments used in this study to measure the opalescence in different biopharmaceutical applications.

Application	Recommended method format	Advantages	Disadvantages
Early-stage characterization & formulation development	Absorbance plate reader	• Low sample volume • Absorbance plate reader are usually available in many laboratories (multi-purpose instrument)	• Low sensitivity, i.e., not suitable for opalescent samples below ca. 10 NTU • Interference with absorbing formulation components
	Microplate nephelometer	• Low sample volume • Very sensitive for large particles (Mie scatterers)	• Strong deviations from conventional nephelometers are expected • Single-purpose instrument
	Dual DLS/SLS plate reader	• Low sample volume • Multi-purpose instrument • Results comparable to common nephelometers for many samples	• Only non-linear calibration successful with polymer standards and no calibration possible with formazin • Insensitive for large particles (Mie scatterers)
Late-stage development and quality control	Non-ratio nephelometer	• Compendial nephelometry according to Pharmacopoeia • Suitable for weakly opalescent samples	• High sample volume • Less suited for highly opalescent samples • Single-purpose instrument
	Ratio-nephelometer	• Compendial nephelometry according to Pharmacopoeia • Suitable for both weakly and highly opalescent samples • Artefact compensation in case of colored samples	• High sample volume • Single-purpose instrument

range that includes highly opalescent samples. The latter might play an important role for the measurements of ATMP samples which are known to be very opalescent.

Finally, bearing the development stage, sample properties, as well as the pitfalls of instrument choice and calibration in mind, opalescence measurements can be a powerful analytical method for the characterization of biopharmaceutical (drug) products in all stages of development.

CRediT authorship contribution statement

Patrick Kunz: Conceptualization, Methodology, Formal analysis, Data curation, Visualization, Project administration. **Eva Stuckenberger:** Investigation, Validation, Visualization. **Kerstin Hausmann:** Investigation, Validation, Visualization. **Lorenzo Gentiluomo:** Methodology, Formal analysis. **Malene Neustrup:** Resources. **Stylianos Michalakis:** Resources. **Ruth Rieser:** Resources. **Stefan Romeijn:** Resources. **Christian Wichmann:** Resources. **Roland Windisch:** Resources. **Andrea Hawe:** Conceptualization, Supervision. **Wim Jiskoot:** Conceptualization, Supervision. **Tim Menzen:** Conceptualization, Writing, Visualization, Supervision.

Declaration of Competing Interest

The authors declare that they have no known competing financial interests or personal relationships that could have appeared to influence the work reported in this paper.

Data availability

The authors are unable or have chosen not to specify which data has been used.

Acknowledgements

We thank Alexandra Roesch (Coriolis Pharma), Johanna Koch (LMU Department of Ophthalmology) and Gerhard Winter (LMU Department of Pharmacy) for their support to the study.

Appendix A. Supplementary data

Supplementary data to this article can be found online at https://doi.org/10.1016/j.ijpharm.2022.122321.

References

AstraZeneca. Vaxzevria, COVID-19 Vaccine (ChAdOx1-S [recombinant]), product information. Annex 1. Summary of product characteristics, 37 pp. https://www.ema.europa.eu/en/documents/product-information/vaxzevria-previously-covid-19-vaccine-astrazeneca-epar-product-information_en.pdf (accessed 28 December 2021).

Barros, M., Zhang, X., Kenrick, S., Valente, J.J., 2021. Opalescence measurements: Improvements in fundamental knowledge, identifying sources of analytical biases, and advanced applications for the development of therapeutic proteins. J Pharm Sci 110, 3550–3557. https://doi.org/10.1016/j.xphs.2021.06.013.

BioNTech. Comirnaty, INN-tozinameran, product information. Annex 1. Summary of product characteristics, 106 pp. https://www.ema.europa.eu/en/documents/product-information/comirnaty-epar-product-information_en.pdf (accessed 28 December 2021).

BioNTech. Factsheet 1 - Comirnaty Production & Ingredients, 2 pp. https://investors.biontech.de/static-files/240d45f5-19a4-46a2-8b28-75697da956b4 (accessed 28 December 2021).

Book of Standards Volume 11.01, 2018. Standard Test Method for Determination of Turbidity Above 1 Turbidity Unit (TU) in Static Mode. ASTM International, West Conshohocken, PA. 10.1520/D7315-17.

0. 10th European Pharmacopoeia (Ph.Eur.10), 10th ed. Deutscher Apotheker Verlag, Stuttgart, 4748 pp.

Gentiluomo, L., Roessner, D., Streicher, W., Mahapatra, S., Harris, P., Frieß, W., 2020. Characterization of Native Reversible Self-Association of a Monoclonal Antibody Mediated by Fab-Fab Interaction. Journal of pharmaceutical sciences 109, 443–451. https://doi.org/10.1016/j.xphs.2019.09.021.

Heuts, J., Varypataki, E.M., van der Maaden, K., Romeijn, S., Drijfhout, J.W., van Scheltinga, A.T., Ossendorp, F., Jiskoot, W., 2018. Cationic Liposomes: A Flexible Vaccine Delivery System for Physicochemically Diverse Antigenic Peptides. Pharmaceutical research 35, 207. https://doi.org/10.1007/s11095-018-2490-6.

ISO/TC 147/SC 2 Physical, chemical and biochemical methods, 2016. Water quality - Determination of turbidity - Part 1: Quantitative methods. ISO. https://www.iso.org/standard/62801.html.

Janssen. COVID-19 Vaccine Janssen, INN-COVID-19 vaccine (Ad26.COV2-S [recombinant]), product information. Annex 1. Summary of product characteristics, 40 pp. https://www.ema.europa.eu/en/documents/product-information/covid-19-vaccine-janssen-epar-product-information_en.pdf (accessed 28 December 2021).

Kingsbury, J.S., 2020. A single molecular descriptor to predict solution behavior of therapeutic antibodies. Science. Advances 6, eabb0372.

Labisch, J.J., Bollmann, F., Wolff, M.W., Pflanz, K., 2021. A new simplified clarification approach for lentiviral vectors using diatomaceous earth improves throughput and safe handling. Journal of biotechnology 326, 11–20. https://doi.org/10.1016/j.jbiotec.2020.12.004.

Mason, B.D., Zhang, L.e., Remmele Jr, R.L., Zhang, J., 2011. Opalescence of an IgG2 monoclonal antibody solution as it relates to liquid-liquid phase separation. Journal of pharmaceutical sciences 100, 4587–4596.

Moderna. Spikevax, dispersion for injection COVID-19 mRNA Vaccine (nucleoside modified), product information. Annex 1. Summary of product information, 32 pp. https://www.ema.europa.eu/en/documents/product-information/spikevax-previously-covid-19-vaccine-moderna-epar-product-information_en.pdf (accessed 28 December 2021).

Münzberg, M., Hass, R., Dinh Duc Khanh, N., Reich, O., 2017. Limitations of turbidity process probes and formazine as their calibration standard. Analytical and bioanalytical chemistry 409, 719–728. 10.1007/s00216-016-9893-1. 2020. Oxford Advanced Learner's Dictionary. 10th Edition.

Raghavan, B., Collins, M., Walls, S., Bergheim-Pietza, S., Alexander, L., 2019. Optimizing the Clarification of Viral Vector Culture for Gene Therapy (A4 Version), Optimizing

the Clarification of Viral Vector Culture for Gene Therapy (A4 Version). Cell & Gene Therapy Insights 5, 1311–1322.
Raut, A.S., Kalonia, D.S., 2015a. Liquid-Liquid Phase Separation in a Dual Variable Domain Immunoglobulin Protein Solution: Effect of Formulation Factors and Protein-Protein Interactions. Molecular pharmaceutics 12, 3261–3271.
Raut, A.S., Kalonia, D.S., 2015b. Opalescence in monoclonal antibody solutions and its correlation with intermolecular interactions in dilute and concentrated solutions. J Pharm Sci 104, 1263–1274. https://doi.org/10.1002/jps.24326.
Raut, A.S., Kalonia, D.S., 2016. Pharmaceutical Perspective on Opalescence and Liquid-Liquid Phase Separation in Protein Solutions. Mol Pharm 13, 1431–1444. https://doi.org/10.1021/acs.molpharmaceut.5b00937.
Rieser, R., Koch, J., Faccioli, G., Richter, K., Menzen, T., Biel, M., Winter, G., Michalakis, S., 2021. Comparison of Different Liquid Chromatography-Based Purification Strategies for Adeno-Associated Virus Vectors. Pharmaceutics 13, 748. https://doi.org/10.3390/pharmaceutics13050748.
Rieser, R., Menzen, T., Biel, M., Michalakis, S., Winter, G., 2022. Systematic Studies on Stabilization of AAV Vector Formulations by Lyophilization. Journal of pharmaceutical sciences. https://doi.org/10.1016/j.xphs.2022.03.004.
Rogers, B.A., Rembert, K.B., Poyton, M.F., Okur, H.I., Kale, A.R., Yang, T., Zhang, J., Cremer, P.S., 2019. A stepwise mechanism for aqueous two-phase system formation in concentrated antibody solutions. Proceedings of the National Academy of Sciences of the United States of America 116, 15784–15791. 10.1073/pnas.1900886116.
Sadar, M. Turbidity Standards. Technical Information Series - Booklet No.12, 18 pp.
Sukumar, M., Doyle, B.L., Combs, J.L., Pekar, A.H., 2004. Opalescent appearance of an IgG1 antibody at high concentrations and its relationship to noncovalent association. Pharmaceutical research 21, 1087–1093.
Usepa, 1993. Method 180.1: Determination of Turbidity by Nephelometry. In: United States Environmental Protection Agency, 2nd ed. www.epa.gov, USA, p. 11 pp..
Yang, T.-C., 2016. Trimerization Dictates Solution Opalescence of a Monoclonal Antibody. Journal of pharmaceutical sciences 105, 2328–2337.